



## Research paper

Identification of dibucaine derivatives as novel potent enterovirus 2C helicase inhibitors: *In vitro*, *in vivo*, and combination therapy study<sup>☆</sup>

Qi Tang<sup>a,1</sup>, Zhichao Xu<sup>b,1</sup>, Mengyu Jin<sup>b,1</sup>, Ting Shu<sup>d</sup>, Yinuo Chen<sup>a</sup>, Leilei Feng<sup>a</sup>,  
 Qiuhan Zhang<sup>a</sup>, Ke Lan<sup>a,c,\*\*</sup>, Shuwen Wu<sup>a,\*\*\*</sup>, Hai-Bing Zhou<sup>b,\*</sup>

<sup>a</sup> State Key Laboratory of Virology, College of Life Sciences, Wuhan University, Wuhan, 430072, China

<sup>b</sup> Hubei Province Engineering and Technology Research Center for Fluorinated Pharmaceuticals, Frontier Science Center for Immunology and Metabolism, Wuhan University School of Pharmaceutical Sciences, Wuhan, 430071, China

<sup>c</sup> Medical Research Institute, Wuhan University, Wuhan, 430071, China

<sup>d</sup> State Key Laboratory of Virology, Wuhan Institute of Virology, Center for Biosafety Mega-Science, Chinese Academy of Sciences, Wuhan, Hubei, 430071, China

## ARTICLE INFO

## Article history:

Received 4 March 2020

Received in revised form

27 March 2020

Accepted 4 April 2020

Available online 25 June 2020

## Keywords:

EV-A71

Structure-activity relationship

2C Helicase inhibitor

Combination therapy

*In vivo* study

## ABSTRACT

Enterovirus A71 (EV-A71) is a human pathogen causing hand, foot and mouth disease (HFMD) which seriously threatened the safety and lives of infants and young children. However, there are no licensed direct antiviral agents to cure the HFMD. In this study, a series of quinoline formamide analogues as effective enterovirus inhibitors were developed, subsequent systematic structure-activity relationship (SAR) studies demonstrated that these quinoline formamide analogues exhibited good potency to treat EV-A71 infection. As described, the most efficient EV-A71 inhibitor **6i** showed good anti-EV-A71 activity ( $EC_{50} = 1.238 \mu\text{M}$ ) in RD cells. Furthermore, compound **6i** could effectively prevent death of virus infected mice at dose of 6 mg/kg. When combined with emetine (0.1 mg/kg), this treatment could completely prevent the clinical symptoms and death of virus infected mice. Mechanism study indicated that compound **6i** inhibited EV-A71 via targeting 2C helicase, thus impeding RNA remodeling and metabolism. Taken together, these data indicated that **6i** is a promising EV-A71 inhibitor and worth extensive pre-clinical investigation as a lead compound.

© 2020 Elsevier Masson SAS. All rights reserved.

## 1. Introduction

Human enteroviruses are a leading source of infants and young children infections mainly caused by EV-A71 and coxsackie virus 16 (CV-A16) with some clinical symptoms including fever, cough, and blisters in the hands, feet, tongue, and oral cavity [1]. These viruses primarily spread through fecal-oral route or may spread via

respiratory droplets and replicate in the respiratory tract [2]. Moreover, HFMD-causing EV-71 is the most virulent serotype [3], which is intimately related to some severe neurological diseases, even leading to death [4,5]. In 1969, the EV-A71 virus was first isolated from a sick child in California [6]. In the next few decades, there are a number of enterovirus-associated HFMD outbreaks reported in Europe and the Asia-Pacific Region [7], causing an estimated 13.7 million cases in China between 2008 and 2015 [3,8]. Recent prevalence of HFMD has seriously threatened the safety and lives of infants and young children. Despite two vaccines (EV-A71C4) have been licensed by Chinese Food and Drug Administration (CFDA) [9,10], however, they do not show cross-protection efficacy against other HFMD pathogens [11]. Moreover, the treatment of severe EV-A71 infection is dependent on supportive treatment and there are no approved direct anti-EV-A71 therapeutics. Thus, there is an urgent need for novel antiviral agents to address the considerable threats and challenges posed by EV-A71 infection.

EV-A71 belongs to the *Picornaviridae* family, and is a non-enveloped and single positive-strand RNA virus containing only one

**Abbreviations:** EV-A71, enterovirus A71; HFMD, foot and mouth disease; SAR, structure-activity relationship; Et<sub>3</sub>N, triethylamine; DMF, dimethylformamide; NaH, sodium hydride; DCM, dichloromethane; KI, potassium iodide; PBS, phosphate-buffer saline.

<sup>☆</sup> Dedicated to the Heroic City of Wuhan

\* Corresponding author.

\*\* Corresponding author. State Key Laboratory of Virology, College of Life Sciences, Wuhan University, Wuhan, 430072, China

\*\*\* Corresponding author.

E-mail addresses: [kulan@whu.edu.cn](mailto:kulan@whu.edu.cn) (K. Lan), [shuwenwu@hotmail.com](mailto:shuwenwu@hotmail.com) (S. Wu), [zhouhb@whu.edu.cn](mailto:zhouhb@whu.edu.cn) (H.-B. Zhou).

<sup>1</sup> Co-first author.

unique large open reading frame (ORF). This ORF yields a single polypeptide that is proteolytically processed into four structural proteins (VP1, VP2, VP3 and VP4), and seven non-structural proteins (2A, 2B, 2C, 3A, 3B, 3C and 3D) [12,13]. These proteins are involved in enteroviruses replication, and each can serve as the target for antiviral agents [14]. Among them, VP1, 2A, 2C, 3A, 3C and 3D<sup>pol</sup> protein are common drug targets. Pleconaril (Fig. 1) exhibited broad spectrum activity against enteroviruses as a capsid protein inhibitor [15,16], specifically inhibiting 90% of rhinoviruses and >99% of enterovirus replication [17]. However, due to the drug–drug interactions with oral contraceptives and insufficient efficacy in treating enterovirus infections, Pleconaril did not progress to registration for rhinovirus-induced common cold [18,19]. Enviroxime (Fig. 1) is a representative compound for the 3A protein and PI4KB inhibitor [20]. Unfortunately, it did not pass the phase II trial due to poor oral bioavailability and vomiting [21,22]. Viral proteinases (2A<sup>pro</sup> and 3C<sup>pro</sup>) optimize virus translation not only by proteolytically processing the viral polypeptide but also cleaving several host proteins. Rupintrivir (Fig. 1), a promising 3C protease inhibitor, has not passed clinical trials because of its poor oral bioavailability [23,24]. On the other hand, the EV-A71 RNA-dependent RNA polymerase (RdRp, 3D<sup>pol</sup>) is also the druggable hotspot which can be targeted by small molecular compounds. For instance, gemcitabine [25], ribavirin and NITD008 (Fig. 1) [26], analogues of nucleoside, could efficiently inhibit EV-A71 infection *in vitro* and *in vivo* by targeting 3D<sup>pol</sup>.

2C is a multi-functional viral protein which is critical for viral replication and encapsidation. It has been reported that 2C not only contributes to PI4KB and lipid droplets recruitment but also binds reticulin 3, an ER (endoplasmic reticulum) protein that facilitates membrane curvature for the formation of replication organelle (RO) [1]. Furthermore, 2C unwinds viral RNA helices, then facilitates the synthesis of EV-A71 RNA in RO; when the function of 2C<sup>ATPase</sup> helicase is damaged, virus replication is mostly interrupted, indicating that 2C<sup>ATPase</sup>-driven RNA remodeling plays an essential role in the viral replication stage [27]. The encapsidation specificity of enterovirus is also governed by 2C-mediated protein–protein interaction in RNA packaging signal. The recent elucidation of crystal structure of EV-A71 2C [28] provides proof for the mechanism of 2C inhibitors, promoting optimization of structure-based drug design. Thus, 2C has been a hotspot to develop anti-enterovirus drugs.

As a part of our long-term interest in the exploration of antiviral agents, some potential antiviral agents with diverse core scaffolds have been designed and synthesized [29,30]. Dibucaine is a FDA approved local anesthetic drug for epidural anesthesia, spinal anesthesia and surface anesthesia. Ulferts et al., firstly identified that dibucaine has a broad activity against enteroviruses by targeting 2C [31]. However, little is known about the structure–activity relationship (SAR) and mechanism of action of this compound for the multi-function of 2C protein. Also, *in vivo* study of this compound is not reported. Considering its potent anti-enterovirus activity, we tried to transform it into an antiviral agent through increasing the antiviral effect and minimizing the adverse effect, and further investigated the mechanism and antiviral efficacy of quinoline formamide analogues in a mouse model. Interestingly, during preparation of manuscript of this study, a series of dibucaine analogues have been developed by Wang et al. with excellent antiviral properties and little side effects [32]. Although this work reported the systematic SAR study of these dibucaine analogues, however, neither the mechanism nor the drug-like study *in vivo* were reported.

In view of the urgent need for antiviral agents to cure the HFMD, also from drug discovery point of view, optimization of quinoline formamide analogues to find suitable lead compound especially with desired drug-like properties, and in-depth mechanistic study of this lead compound seem necessary. In this study, we modified the length of the alkoxy chain and various substituents of amino moiety based on the quinoline formamide skeleton of dibucaine **6d** by the guide of SAR study of these compounds and the structural biology study of EV-A71 2C protein (Fig. 2). The systematic SAR study indicated that compound **6i** exhibited great efficacy on anti-EV-A71 activity *in vitro*. On the other hand, primary mechanism study showed that the most effective compound **6i** is an oral inhibitor of enterovirus 2C helicase with effective anti-EV-A71 activity in mice. It is worth mentioned that the combination treatment with previously reported EV-A71 inhibitor emetine [33] could achieved complete protection. Taken together, we reported a series of quinoline formamides as novel potent EV-A71 inhibitors with desired drug-like properties, exemplified by **6i**.

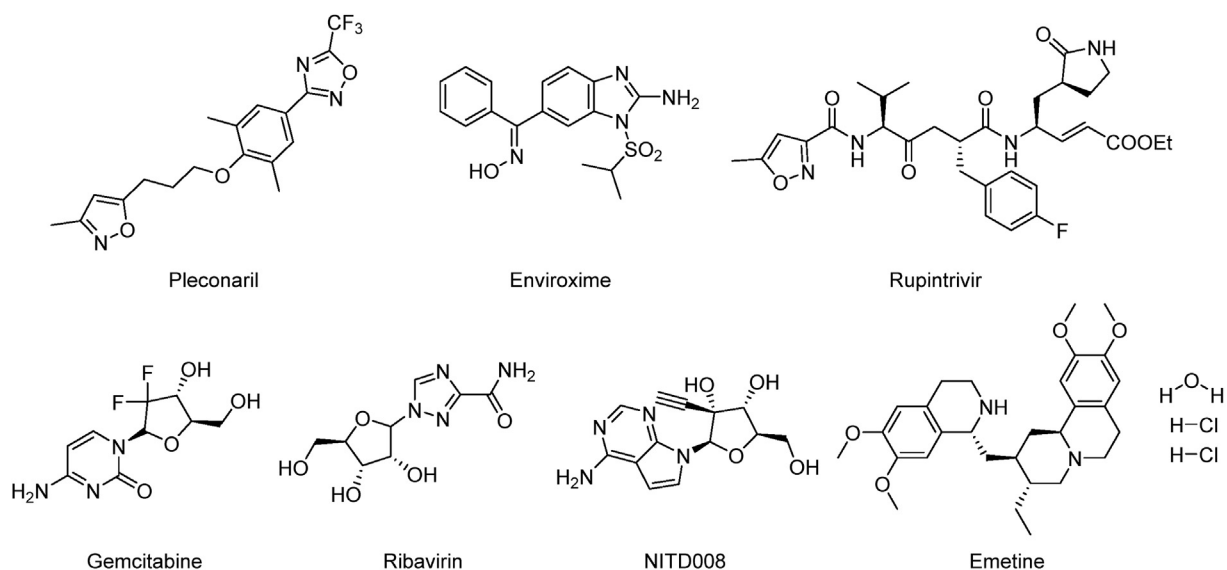
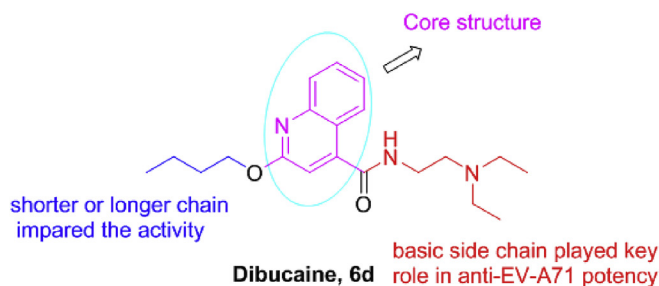


Fig. 1. Representative chemical structures of reported enterovirus inhibitors.

## i) SAR Optimization



## ii) Mechanism and Drug-like Property Study

- Lead compound **6i**: EC<sub>50</sub> = 1.238 μM; CC<sub>50</sub> = 105.679 μM; SI = 85.4
- 2C helicase inhibitory activity
- Orally effective in mice
- Combination treatment with emetine achieved complete protection

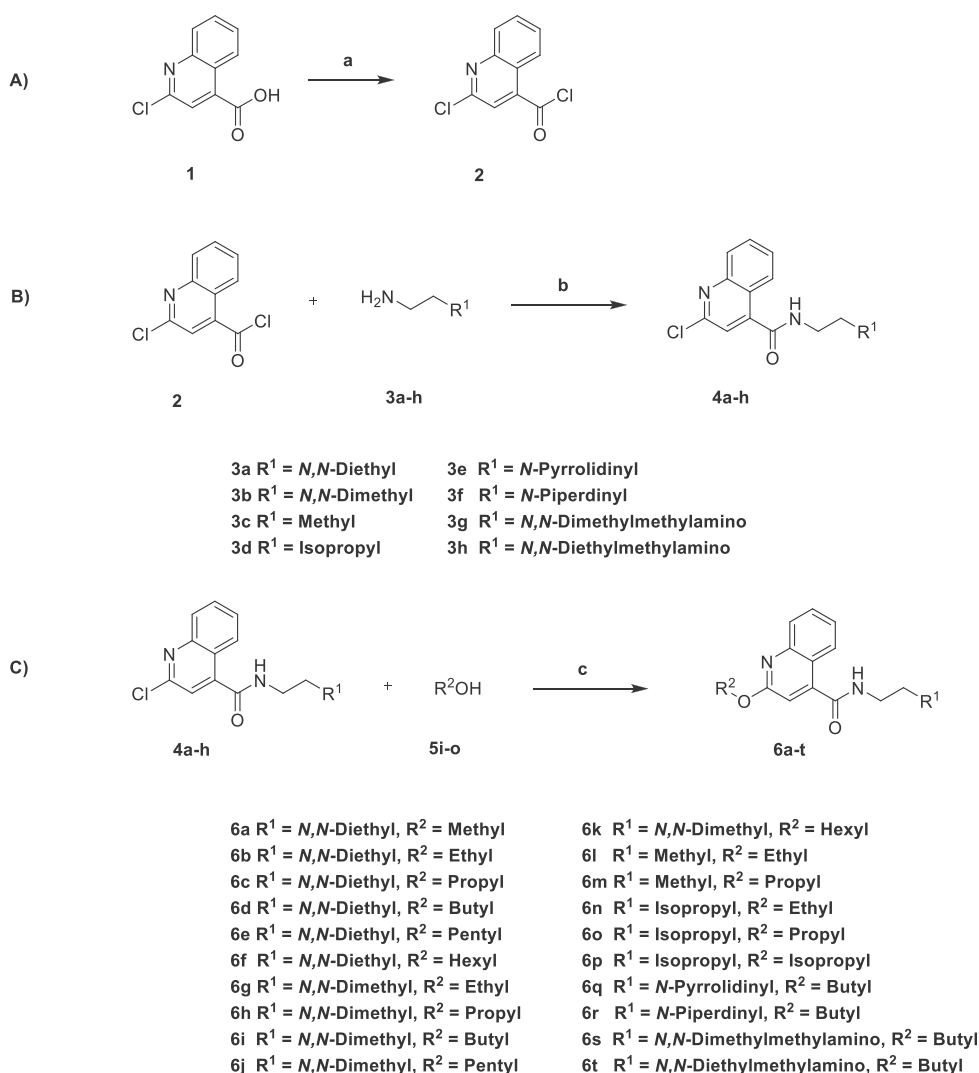
Fig. 2. SAR optimization based on dibucaine structure and further drug-like studies.

## 2. Results and discussion

## 2.1. Chemistry

The synthesis of quinoline formamide derivatives was shown in Scheme 1. Firstly, we utilized 2-chloroquinoline-4-carboxylic acid **1**

and thionyl chloride to generate intermediate **2**, which was selected for the reaction of next step. Intermediates **4a-h** were synthesized by amidation of acyl chloride **2** and amines **3a-h**. Then, intermediates **4a-h** were reacted with different alcohols **5i-o** through substitution reaction under the protection of argon to produce target compounds **6a-t**.



Scheme 1. Synthesis of quinoline formamide derivatives **6a-t**.

<sup>a</sup>Reagents and conditions: (a) SOCl<sub>2</sub> (2.5 eq), DCM, reflux, 4 h; (b) Et<sub>3</sub>N (1.2 eq), DCM, rt, overnight; (c) NaH (2.7 eq), KI, DMF, 80 °C, 72 h.

## 2.2. Biological testing

### 2.2.1. Biological activity of dibucaine derivatives against EV-A71

All synthesized quinoline formamide analogues were evaluated for their biological activity against EV-A71 in RD cells while enviroxime was chosen for positive control. The results were summarized in Table 1 and SAR of these dibucaine derivatives were investigated.

From the activity comparison of **6a-f**, we can see that when the length of carbon chain was 2–4, it showed a better anti-EV-A71 activity with low micromolar values. Then when *N,N*-diethyl group was transformed into *N,N*-dimethyl moiety, these modified new derivatives exhibited better activity against EV-A71 (**6h-k** vs **6c-f** respectively) except for ethyl group substituted at the R<sup>2</sup> position. Among them, compound **6i** with *N,N*-dimethyl moiety substituted at R<sup>1</sup> and *n*-butyl group substituted at R<sup>2</sup> displayed the best activity of 1.238  $\mu$ M against EV-A71 infection in RD cells.

In order to develop an in-depth study of R<sup>1</sup> substituents, we did the following modifications: (1) replacing the substituents of R<sup>1</sup> with alkyl groups; (2) modifying the *N,N*-dimethyl group with *N*-containing rings; (3) extending the length of the carbon chain.

It can be observed that the activities of **6l-p** were markedly decreased when R<sup>1</sup> was changed to alkyl groups like methyl or propyl substituents. Both **6q** and **6r** of *N*-containing rings exhibited comparable efficacy with **6i**. While the length of carbon chain was increased, the anti-EV-A71 activity was severely impeded. Hence, we selected **6i** for further study on the mechanism of action as EV-A71 inhibitors.

### 2.2.2. Compound **6i** efficiently inhibited EV-A71 replication in vitro

As described above, compound **6i** showed the best potency against EV-A71. Then we utilized plaque assay, Western blot and immunofluorescence assays to further evaluate the antiviral efficacy of **6i**, respectively. As shown in Fig. 3A, compound **6i** could robustly suppress EV-A71 replication in RD cell model. We also found that compound **6i** could down-regulated the expression of VP1 by immunofluorescence assay dose-dependently (Fig. 3B). Consistent with the immunofluorescence results, compound **6i** could efficiently inhibit the expression of viral 2C and VP1 (Fig. 3C). These results indicated that compound **6i** robustly block EV-A71 replication in cell culture assays.

### 2.2.3. Time-of-addition experiment

The antiviral activity of dibucaine was firstly identified in screening of drug libraries, however, the activity studies were rather limited [34]. Ulferts et al. has reported that dibucaine inhibited enterovirus by targeting 2C [31]. However, the enteroviral 2C is a multi-functional protein participating in viral life cycle and the antiviral mechanism of dibucaine need to be further elucidated. To assess which stage of EV-A71 infection compound **6i** inhibited, we conducted time-course experiment in the case of EV-A71 infection. The EV-A71 infected cells were treated with compound **6i** and enviroxime at indicated times following viral absorption. To investigate viral protein expression, viral RNA level and viral genome copies in cell lysates or supernatants were harvested at 12 hpi, Western blot assay and qRT-PCR were conducted. For the treatment of compound **6i**, inhibition rates before 4 h showed nearly 100% in infected cells (Fig. 4A, B, C). We also observed that similar results when treated with enviroxime. The time-course assay result showed that compound **6i** exhibited antiviral efficacy during the early stage of the EV-A71 life cycle.

### 2.2.4. Compound **6i** inhibited EV-A71 2C helicase

It was reported that ALA-224, ALA-229 and ILE-227 in 2C was associated with the resistance to dibucaine [31]. The ALA-224 in 2C

of EV-D68, CV-A16, CV-B3 and Echov-E7 is identical but in EV-A71 it is not; and ALA-229 is conservative only in CV-B3, EV-D68 and Echov-E7. The ILE-227 in 2C helicase SF3 motif is conservative in all the selected enteroviruses in Fig. S1. To investigate whether compound **6i** interacts with 2C in helicase SF3 motif, the dsRNA unwinding in cells by 2C was investigated. The results showed that the viral RNA helices were dramatically unwound at 10 hpi (Fig. 5A) and mostly unwound at 12 hpi (data not shown) during EV-A71 replication without treatment; and compound **6i** could dramatically inhibit the dsRNA unwinding and increase accumulation of dsRNA and 2C complex in RD cells (Fig. 5A and B). Enviroxime, a PI4KB inhibitor which is critical for the viral RO formation and viral replication did not inhibit the unwinding of dsRNA. To investigate the action mechanism underlying the blocking of helix unwinding activity of compound **6i**, we investigated whether compound **6i** could directly impede the activity of helicase. MBP-fusion EV-A71 2C<sup>ATPase</sup> helicase reaction mixture with compound **6i** or DMSO as described was detected via gel electrophoresis (Fig. S2A) [27]. Compound **6i** decreased the activity of helicase *in vitro* in dose-dependent manner as shown in Fig. S2B. These results indicated that compound **6i** inhibit EV-A71 replication by impeding the EV-A71 2C<sup>ATPase</sup>-mediated RNA remodeling.

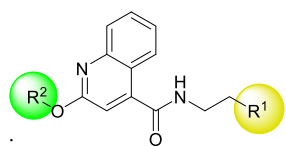
### 2.3. Oral efficacy against EV-A71 infection of compound **6i**

In line with the *in vitro* activity of the quinoline formamide analogues, oral administration of compound **6i** protected mice from lethal challenge of EV-A71 GZ-CII. When compound **6i** was orally administrated at doses of 4 and 6 mg/kg twice daily, initiated 6 h before challenge and lasting for 4 days, resulted in 30% and 67% survival at day 14 in comparison to the vehicle group, in which showed 30% survival (Fig. 6A). Doses of 6 mg/kg of compound **6i** not only efficiently decreased the morbidity and mortality, but also alleviated the clinical EV-A71 symptoms (Fig. 6B); the dose of 4 mg/kg of compound **6i** only delayed death of EV-A71 infected mice (Fig. 6A). To investigate the adverse effect of compound **6i**, 14-day sucking mice were orally administrated with vehicle or compound **6i** twice daily for successive 4 days, and then were observed continuing for two weeks. Compared to the mock (non-treated) group mice, there is no significant difference between treated and no-treated mice in weight growth (Fig. 6C). To further investigate the antiviral activity *in vivo*, combination treatment was assessed. When combining the treatment with emetine, a viral internal ribosome entry site (IRES) inhibitor [33], it can completely prevent death and disease of EV-A71 infected mice (Fig. 6D and E). These results indicate that compound **6i** is a promising EV-A71 inhibitor with oral activity and little side effect in mice.

### 2.4. Molecular docking

We have identified the compound **6i** could inhibit the replication of virus by impairing 2C helicase activity. To fully understand the binding mode of **6i** with EV-A71 2C protein, the molecular modeling study was conducted based on the crystal structure of 2C protein (PDB 5GQ1) by using AutoDock Vina [28,29]. In Fig. 7A, one can see that compound **6i** could form five hydrogen bonds with the residues ASP-177, LYS-135, SER-136, GLY-132. Among them, there were two hydrogen bonds existed between compound **6i** and LYS-135. More specifically, the oxygen atom and the amide hydrogen of carboxamide group in compound **6i** formed two hydrogen bonds with the amino group of LYS-135 and carboxyl group of ASP177, respectively. The nitrogen atom in quinoline moiety formed a hydrogen bond with the amino group of GLY-132. Moreover, two hydrogen bonds were identified between the oxygen atom of butoxy in **6i** with the amide hydrogens of LYS-135 and SER-136,

**Table 1**  
Biological Evaluation of the quinoline formamide analogues against EV-A71 Virus<sup>a</sup>.



Entry	Cmpd	R <sup>1</sup>	R <sup>2</sup>	RD cell		SI <sup>d</sup>
				EC <sub>50</sub> (μM) <sup>b</sup>	CC <sub>50</sub> (μM) <sup>c</sup>	
1	<b>6a</b>			27.650 ± 0.068	>110.599	>4.0
2	<b>6b</b>			2.477 ± 0.300	>105.679	>42.7
3	<b>6c</b>			2.371 ± 0.130	>101.182	>42.7
4	<b>6d</b>			2.275 ± 0.085	>97.049	>42.7
5	<b>6e</b>			5.828 ± 0.172	34.965	6.0
6	<b>6f</b>			4.206 ± 0.127	33.645	8.0
7	<b>6g</b>			3.625 ± 0.192	115.999	31.9
8	<b>6h</b>			1.581 ± 0.115	>110.599	>70.0
9	<b>6i</b>			1.238 ± 0.122	105.679	85.4
10	<b>6j</b>			1.581 ± 0.092	75.886	48.0
11	<b>6k</b>			2.275 ± 0.061	36.393	16.0
12	<b>6l</b>			2.016 ± 0.184	>70.238	>34.8
13	<b>6m</b>			>100	ND <sup>e</sup>	f
14	<b>6n</b>			>100	ND <sup>e</sup>	f
15	<b>6o</b>			58.198 ± 1.781	87.297	1.5
16	<b>6p</b>			58.198 ± 2.627	>116.395	>2.0
17	<b>6q</b>			1.525 ± 0.103	>97.692	>64.1
18	<b>6r</b>			1.465 ± 0.190	93.770	64.0
19	<b>6s</b>			>100	ND <sup>e</sup>	f
20	<b>6t</b>			>100	ND <sup>e</sup>	f
21	<b>Enviroxime</b>	—	—	0.140 ± 0.010	28.0	200.0

<sup>a</sup> CC<sub>50</sub> or EC<sub>50</sub> data are means of triplicates SD and one representative dataset of at least three independent experiments is shown.

<sup>b</sup> EC<sub>50</sub>: effective concentration (μM) to inhibit 50% virus replication, represented the mean ± SD.

<sup>c</sup> CC<sub>50</sub>: cytotoxic concentration (μM) for 50% cell death.

<sup>d</sup> SI: Selectivity Index (CC<sub>50</sub>/EC<sub>50</sub>).

<sup>e</sup> ND: not determined.

<sup>f</sup> Not calculated.

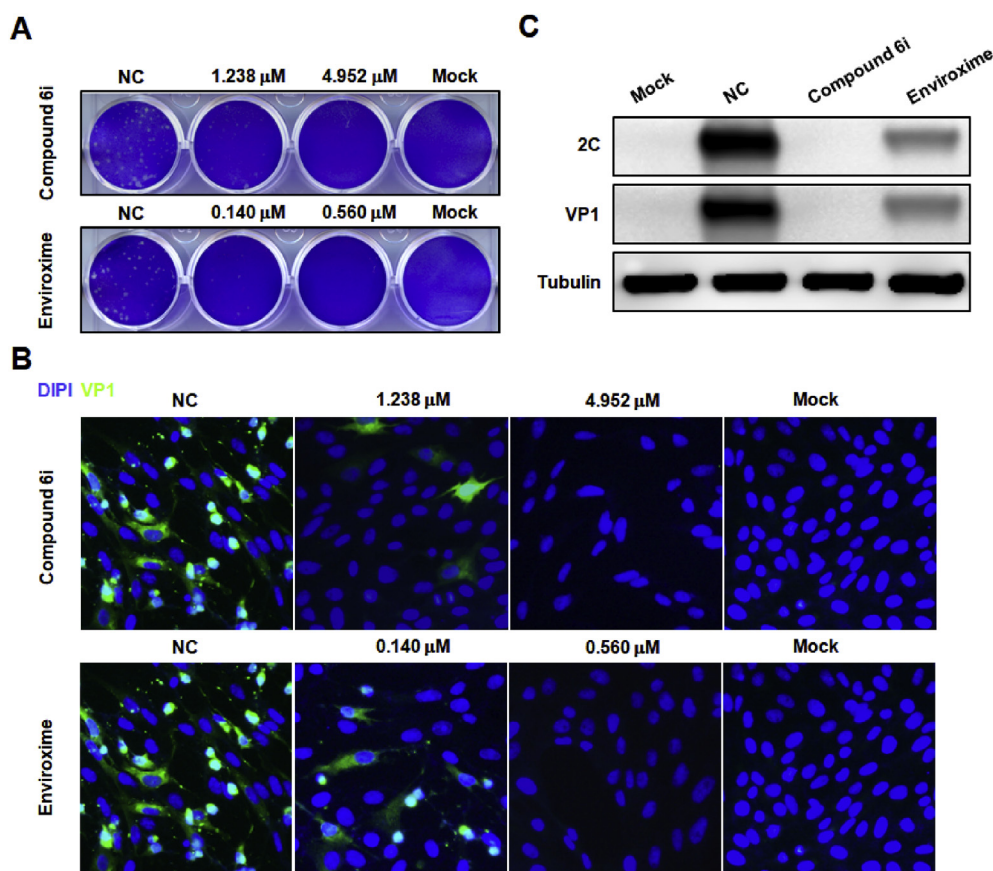


**Fig. 3.** Anti-EV-A71 activity of compound **6i**. (A) Compound **6i** inhibited the proliferation of EV-A71. In plaque assay, RD cells were infected with EV-A71 at 0.0005 MOI, then treated with compound **6i** or enviroxime and 0.75% low melting-point agarose for 48 h at 1 hpi. (B) Antiviral effect was further confirmed by immunofluorescence assay in Vero cells. (C) Compound **6i** dramatically inhibited the expression of viral protein VP1 and 2C compared to that with non-treated in RD cells. For immunofluorescence assay and Western blot assay, cells were infected with EV-A71 at 1 MOI, then treated with indicated compound **6i** or enviroxime at 1 hpi. Cells were fixed or harvested for immunofluorescence assay or Western blot assay at 24 hpi.

respectively. As Fig. 7B showed, **6i** occupied the cavity of the protein in a semi-closed mode. Except for the five hydrogen bonds, hydrophobic interaction was observed in the hydrophobic pocket which was formed by residues LEU-261, ALA-263, LEU-137, PRO-131, and PRO-159. Also, a  $\pi$ - $\pi$  interaction was determined in quinoline parts of **6i** with the tetrahydropyrrole moiety of PRO-131, which might make a contribution to the enhanced binding force and inhibitory activity.

### 3. Conclusions

In summary, in this study, various of dibucaine derivatives were synthesized and their biological activities against EV-A71 were evaluated. These quinoline formamide analogues exhibited good anti-EV-A71 activity and induced a low cytotoxicity in RD cells. Subsequent SAR studies demonstrated that the nitrogen-substituted groups at R<sup>1</sup> played crucial roles in inhibition of virus replication. A preliminary mechanistic study indicated that these derivatives inhibited enterovirus replication through blocking the helicase activity of 2C which could remodel RNA structures and/or RNA-protein interactions. *In vivo* study showed that **6i** was orally active and without significant toxicity in mice. The combination treatment with 0.1 mg/kg emetine in EV-A71 infected mice could completely prevent clinical symptoms and death. Actually, there are few effective direct anti-EV-A71 agents *in vivo* reported, and here we provide an in-depth study about druggability properties of these quinoline formamide analogues based on dibucaine scaffold.

Therefore, these quinoline formamide derivatives could serve as the candidate to develop new anti-EV-A71 drugs.

## 4. Experimental section

### 4.1. Materials and methods

All chemical materials and dry solvents such as DMF and DCM were purchased from reagent companies and used directly. Reactions were monitored by TLC or GCMS-TQ8040 and all target compounds were obtained by flash column methodology. <sup>1</sup>H NMR and <sup>13</sup>C NMR spectra were tested by Bruker AV400 instrument. Tetramethylsilane was used as the standard to report chemical shifts. X-4 Beijing Tech melting point apparatus were applied for measuring melting points. All final compounds showed >95% purity which was confirmed by HPLC.

### 4.2. Chemistry

#### 4.2.1. Procedure for the synthesis of acyl chloride **2**

2-chloroquinoline-4-carboxylic acid **1** (0.482 mmol) was dissolved in DCM (5 mL), then thionyl chloride (0.088 mL) was added. The mixture was kept at 55 °C for 4 h. When the reaction was completed, removed the solvent and carried out the next reaction.

#### 4.2.2. General procedure to synthesize intermediate **4a-h**

Amine (**3a-h**) (0.530 mmol) was added into DCM (5 mL) with

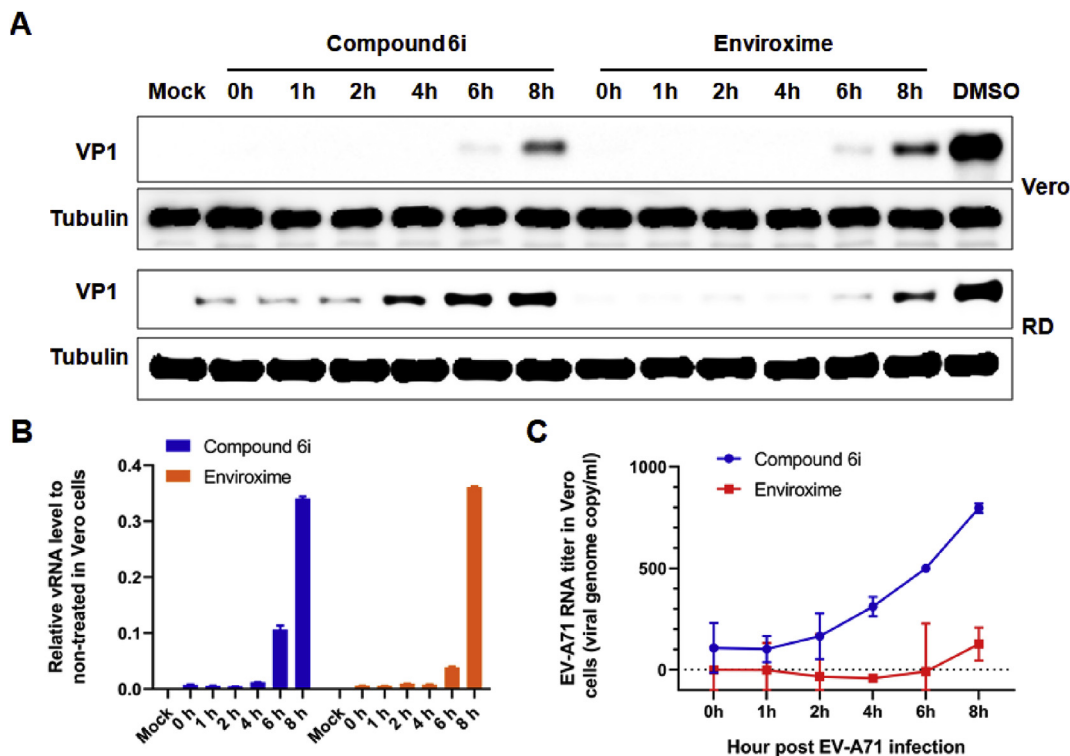


**Fig. 4.** The action stage of compound **6i** and enviroxime was confirmed by time-of-addition assay. The EV-A71 infected RD or Vero cells (1 MOI) were treated with compound **6i** or enviroxime at 3.2  $\mu$ M and 0.56  $\mu$ M, respectively, at indicated time points and harvested at 12 hpi as shown in the Experimental section. (A) Western blot was used to assess the abundance of VP1 expression with compound **6i**, enviroxime, DMSO. (B, C) The EV-A71 RNA accumulation in cells or in supernatants of the treated or untreated cases with **6i** or enviroxime were investigated by qRT-PCR, respectively. These representative data were obtained by at least two independent experiments with standard errors.

0.1 mL Et<sub>3</sub>N at 0 °C. Next, the acyl chloride **2** was added slowly to the mixture while the temperature maintained at 0 °C. Removed the ice and kept on room temperature overnight. Quenched the reaction, extracted with water and ethyl acetate, then concentrated. Finally, flash column chromatography was applied to purified the residue to get the intermediate **4a-h**.

#### 4.2.3. General procedure to synthesize quinoline formamides **6a-t**

First, sodium hydride was reacted with alcohols **5i-o** to produce sodium alkoxide under the protection of argon. After 30 min, a DMF solution of intermediates **4a-h** and potassium iodide was added into the mixture above. The reaction was kept at 80 °C for 3 days. Then quenched the reaction with water, extracted with water and ethyl acetate, then concentrated. Finally, flash column chromatography was applied to purified the residue to obtain the final product **6a-t**.

#### 4.2.4. Characterization data for final compounds **6a-t**

**4.2.4.1. N-(2-(Diethylamino)ethyl)-2-methoxyquinoline-4-carboxamide (6a).** Yellow solid, 77.1% yield, mp 112–113 °C. <sup>1</sup>H NMR (400 MHz, CDCl<sub>3</sub>)  $\delta$  8.14 (d, *J* = 8.3 Hz, 1H), 7.88 (d, *J* = 8.3 Hz, 1H), 7.70–7.57 (m, 1H), 7.41 (t, *J* = 7.6 Hz, 1H), 6.97 (s, 1H), 6.88 (s, 1H), 4.09 (s, 3H), 3.56 (q, *J* = 5.6 Hz, 2H), 2.68 (t, *J* = 6.0 Hz, 2H), 2.56 (q, *J* = 7.1 Hz, 4H), 1.02 (t, *J* = 7.2 Hz, 6H). <sup>13</sup>C NMR (100 MHz, CDCl<sub>3</sub>)  $\delta$  167.0, 161.7, 147.2, 145.2, 130.0, 127.6, 125.4, 124.7, 121.6, 111.0, 53.6, 51.2, 46.6, 37.3, 11.8. HRMS (ESI) calcd for C<sub>17</sub>H<sub>23</sub>N<sub>3</sub>O<sub>2</sub> [M+H]<sup>+</sup> 302.1863, found 302.1856.

**4.2.4.2. N-(2-(Diethylamino)ethyl)-2-ethoxyquinoline-4-carboxamide (6b).** Yellow solid, 45.3% yield, mp 122–124 °C. <sup>1</sup>H NMR (400 MHz, CDCl<sub>3</sub>)  $\delta$  8.15 (d, *J* = 8.3 Hz, 1H), 7.86 (d, *J* = 8.4 Hz, 1H), 7.66 (t, *J* = 7.6 Hz, 1H), 7.42 (t, *J* = 7.6 Hz, 1H), 6.98 (s, 1H), 6.79

(s, 1H), 4.56 (q, *J* = 7.1 Hz, 2H), 3.59 (q, *J* = 5.5 Hz, 2H), 2.70 (t, *J* = 6.0 Hz, 2H), 2.57 (q, *J* = 7.1 Hz, 4H), 1.47 (t, *J* = 7.1 Hz, 3H), 1.03 (t, *J* = 7.1 Hz, 6H). <sup>13</sup>C NMR (100 MHz, CDCl<sub>3</sub>)  $\delta$  167.0, 161.4, 147.3, 145.1, 129.9, 127.6, 125.3, 124.6, 121.6, 111.2, 62.0, 51.2, 46.6, 37.4, 14.6, 11.7. HRMS (ESI) calcd for C<sub>18</sub>H<sub>25</sub>N<sub>3</sub>O<sub>2</sub> [M+H]<sup>+</sup> 316.2020, found 316.2013.

**4.2.4.3. N-(2-(Diethylamino)ethyl)-2-propoxyquinoline-4-carboxamide (6c).** Yellow solid, 37.1% yield, mp 82–84 °C. <sup>1</sup>H NMR (400 MHz, CDCl<sub>3</sub>)  $\delta$  8.12 (d, *J* = 8.3 Hz, 1H), 7.85 (d, *J* = 8.4 Hz, 1H), 7.64 (t, *J* = 7.7 Hz, 1H), 7.40 (t, *J* = 7.6 Hz, 1H), 6.97 (s, 1H), 6.89 (s, 1H), 4.44 (t, *J* = 6.7 Hz, 2H), 3.56 (q, *J* = 5.6 Hz, 2H), 2.67 (t, *J* = 6.0 Hz, 2H), 2.56 (q, *J* = 7.1 Hz, 4H), 1.88–1.82 (m, 2H), 1.07 (t, *J* = 7.4 Hz, 3H), 1.01 (t, *J* = 7.1 Hz, 6H). <sup>13</sup>C NMR (100 MHz, CDCl<sub>3</sub>)  $\delta$  167.1, 161.6, 147.3, 145.1, 129.9, 127.6, 125.3, 124.5, 121.6, 111.2, 67.8, 51.2, 46.6, 37.3, 22.3, 11.7, 10.6. HRMS (ESI) calcd for C<sub>19</sub>H<sub>27</sub>N<sub>3</sub>O<sub>2</sub> [M+H]<sup>+</sup> 330.2176, found 330.2168.

**4.2.4.4. 2-Butoxy-N-(2-(diethylamino)ethyl)quinoline-4-carboxamide (6d).** Yellow solid, 44.4% yield, mp 78–79 °C. <sup>1</sup>H NMR (400 MHz, CDCl<sub>3</sub>)  $\delta$  8.14 (d, *J* = 8.4 Hz, 1H), 7.87 (d, *J* = 8.4 Hz, 1H), 7.66 (t, *J* = 7.6 Hz, 1H), 7.42 (t, *J* = 7.6 Hz, 1H), 6.98 (s, 1H), 6.78 (s, 1H), 4.50 (t, *J* = 6.7 Hz, 2H), 3.59 (q, *J* = 5.6 Hz, 2H), 2.70 (t, *J* = 6.0 Hz, 2H), 2.58 (q, *J* = 7.1 Hz, 4H), 1.91–1.73 (m, 2H), 1.61–1.45 (m, 2H), 1.03 (t, *J* = 7.1 Hz, 9H). <sup>13</sup>C NMR (100 MHz, CDCl<sub>3</sub>)  $\delta$  167.1, 161.6, 147.3, 145.1, 129.9, 127.6, 125.3, 124.6, 121.6, 111.2, 66.0, 51.2, 46.6, 37.4, 31.0, 19.3, 13.9, 11.7. HRMS (ESI) calcd for C<sub>20</sub>H<sub>29</sub>N<sub>3</sub>O<sub>2</sub> [M+H]<sup>+</sup> 344.2333, found 344.2327.

**4.2.4.5. N-(2-(Diethylamino)ethyl)-2-(pentyl)oxyquinoline-4-carboxamide (6e).** Yellow solid, 12.4% yield, mp 85–86 °C. <sup>1</sup>H NMR (400 MHz, CDCl<sub>3</sub>)  $\delta$  8.12 (d, *J* = 8.4 Hz, 1H), 7.85 (d, *J* = 8.5 Hz, 1H),

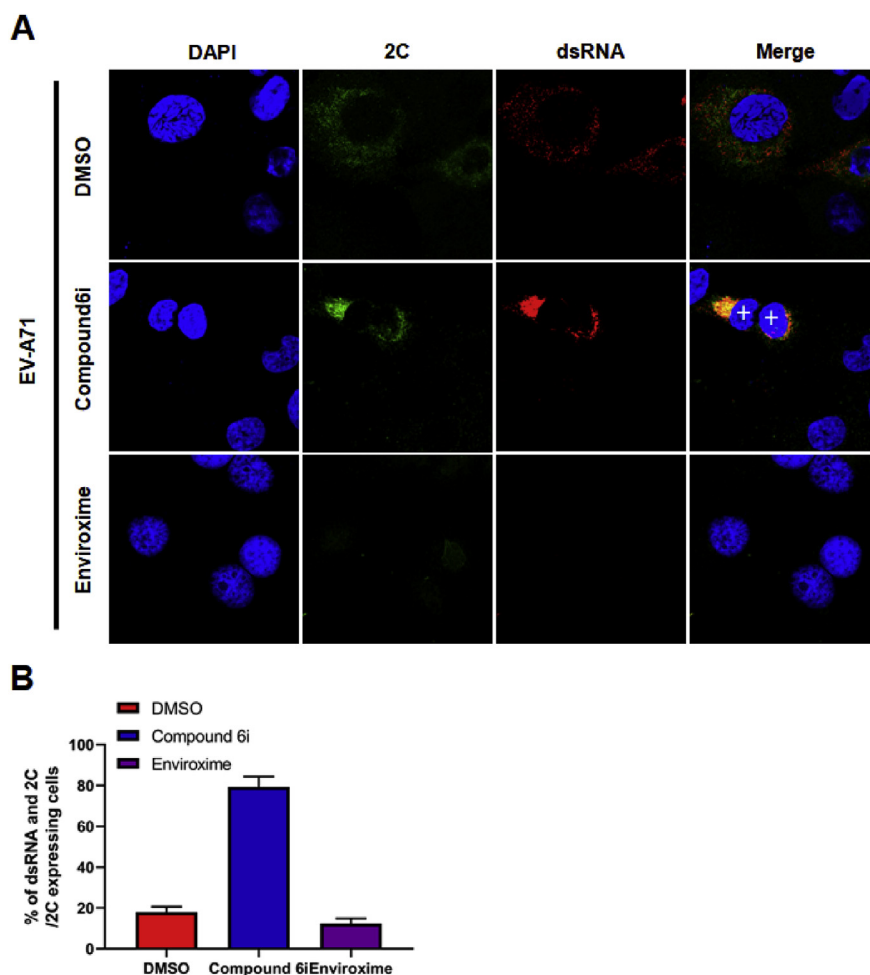


**Fig. 5.** Compound **6i** inhibited the unwinding of viral RNA helices. (A) The location of DAPI, 2C, and dsRNA in EV71-infected RD cells (10 MOI) at 10 hpi with treatment of DMSO, Enviroxime (0.56  $\mu$ M) and Compound **6i**-treated (4.95  $\mu$ M) at 8 hpi, respectively. (B) Quantitative analysis of cells with dsRNA and 2C co-location/2C expressing cells. Co-location was marked by 2C or dsRNA.  $n = 5$ , 00 cells/condition were counted, mean  $\pm$  SD.

7.63 (t,  $J = 7.7$  Hz, 1H), 7.39 (t,  $J = 7.6$  Hz, 1H), 7.13 (s, 1H), 6.97 (s, 1H), 4.47 (t,  $J = 6.7$  Hz, 2H), 3.67–3.52 (m, 2H), 2.76 (t,  $J = 5.3$  Hz, 2H), 2.64 (q,  $J = 7.0$  Hz, 4H), 1.83 (m, 2H), 1.57–1.36 (m, 4H), 1.05 (t,  $J = 7.1$  Hz, 6H), 0.95 (t,  $J = 6.9$  Hz, 3H).  $^{13}$ C NMR (100 MHz,  $\text{CDCl}_3$ )  $\delta$  167.2, 161.6, 147.3, 144.9, 129.9, 127.6, 125.3, 124.5, 121.5, 111.3, 66.3, 51.2, 46.7, 37.1, 28.6, 28.3, 22.5, 14.0, 11.3. HRMS (ESI) calcd for  $\text{C}_{21}\text{H}_{31}\text{N}_3\text{O}_2$  [ $\text{M}+\text{H}$ ] $^+$  358.2489, found 358.2486.

**4.2.4.6. N-(2-(Diethylamino)ethyl)-2-(hexyloxy)quinoline-4-carboxamide (6f).** Yellow solid, 12.0% yield, mp 78–79  $^\circ\text{C}$ .  $^1\text{H}$  NMR (400 MHz,  $\text{CDCl}_3$ )  $\delta$  8.13 (d,  $J = 8.3$  Hz, 1H), 7.86 (d,  $J = 8.3$  Hz, 1H), 7.64 (d,  $J = 16.6$  Hz, 1H), 7.41 (t,  $J = 7.1$  Hz, 1H), 6.97 (s, 1H), 6.81 (s, 1H), 4.48 (t,  $J = 6.7$  Hz, 2H), 3.57 (q,  $J = 5.6$  Hz, 2H), 2.68 (t,  $J = 6.0$  Hz, 2H), 2.57 (q,  $J = 7.1$  Hz, 4H), 1.88–1.80 (m, 2H), 1.55–1.45 (m, 2H), 1.42–1.33 (m, 4H), 1.02 (t,  $J = 7.1$  Hz, 6H), 0.93 (t,  $J = 6.9$  Hz, 3H).  $^{13}$ C NMR (100 MHz,  $\text{CDCl}_3$ )  $\delta$  167.1, 161.6, 147.3, 145.1, 129.9, 127.6, 125.3, 124.6, 121.6, 111.2, 66.3, 51.2, 46.6, 37.4, 31.6, 28.9, 25.8, 22.6, 14.1, 11.7. HRMS (ESI) calcd for  $\text{C}_{22}\text{H}_{33}\text{N}_3\text{O}_2$  [ $\text{M}+\text{H}$ ] $^+$  372.2646, found 372.2638.

**4.2.4.7. N-(2-(Dimethylamino)ethyl)-2-ethoxyquinoline-4-carboxamide (6g).** White solid, 16.7% yield, mp 159–161  $^\circ\text{C}$ .  $^1\text{H}$  NMR (400 MHz,  $\text{CDCl}_3$ )  $\delta$  8.13 (d,  $J = 8.2$  Hz, 1H), 7.85 (d,  $J = 8.4$  Hz, 1H), 7.64 (t,  $J = 7.6$  Hz, 1H), 7.41 (t,  $J = 7.6$  Hz, 1H), 6.97 (s, 1H), 6.83 (s, 1H), 4.55 (q,  $J = 7.1$  Hz, 2H), 3.59 (q,  $J = 5.6$  Hz, 2H), 2.55 (t,  $J = 6.0$  Hz,

2H), 2.26 (s, 6H), 1.46 (t,  $J = 7.1$  Hz, 3H).  $^{13}$ C NMR (100 MHz,  $\text{CDCl}_3$ )  $\delta$  167.2, 161.3, 147.3, 144.9, 130.0, 127.6, 125.3, 124.6, 121.6, 111.2, 62.0, 57.5, 45.1, 37.2, 14.5. HRMS (ESI) calcd for  $\text{C}_{16}\text{H}_{21}\text{N}_3\text{O}_2$  [ $\text{M}+\text{H}$ ] $^+$  288.1707, found 288.1701.

**4.2.4.8. N-(2-(Dimethylamino)ethyl)-2-propoxyquinoline-4-carboxamide (6h).** Yellow solid, 12.3% yield, mp 126–128  $^\circ\text{C}$ .  $^1\text{H}$  NMR (400 MHz,  $\text{CDCl}_3$ )  $\delta$  8.12 (d,  $J = 8.3$  Hz, 1H), 7.91–7.81 (m, 1H), 7.64 (t,  $J = 7.7$  Hz, 1H), 7.41 (t,  $J = 7.6$  Hz, 1H), 6.99 (s, 1H), 6.80 (s, 1H), 4.45 (t,  $J = 6.7$  Hz, 2H), 3.62–3.56 (m, 2H), 2.55 (t,  $J = 5.8$  Hz, 2H), 2.26 (s, 6H), 1.92–1.80 (m, 2H), 1.08 (t,  $J = 7.4$  Hz, 3H).  $^{13}$ C NMR (100 MHz,  $\text{CDCl}_3$ )  $\delta$  167.2, 161.5, 147.3, 144.9, 130.0, 127.6, 125.3, 124.6, 121.6, 111.2, 67.8, 57.5, 45.1, 37.2, 22.3, 10.6. HRMS (ESI) calcd for  $\text{C}_{17}\text{H}_{23}\text{N}_3\text{O}_2$  [ $\text{M}+\text{H}$ ] $^+$  302.1863, found 302.1856.

**4.2.4.9. 2-Butoxy-N-(2-(dimethylamino)ethyl)quinoline-4-carboxamide (6i).** Yellow solid, 40.9% yield, mp 120–122  $^\circ\text{C}$ .  $^1\text{H}$  NMR (400 MHz,  $\text{CDCl}_3$ )  $\delta$  8.14 (d,  $J = 8.3$  Hz, 1H), 7.86 (d,  $J = 8.5$  Hz, 1H), 7.66 (t,  $J = 7.7$  Hz, 1H), 7.43 (t,  $J = 8.1$  Hz, 1H), 6.99 (s, 1H), 6.73 (s, 1H), 4.50 (t,  $J = 6.7$  Hz, 2H), 3.66–3.56 (m, 2H), 2.56 (t,  $J = 5.9$  Hz, 2H), 2.27 (s, 6H), 1.92–1.76 (m, 2H), 1.63–1.46 (m, 2H), 1.02 (t,  $J = 7.4$  Hz, 3H).  $^{13}$ C NMR (100 MHz,  $\text{CDCl}_3$ )  $\delta$  167.1, 161.5, 147.3, 144.9, 129.9, 127.6, 125.3, 124.6, 121.6, 111.2, 66.0, 57.5, 45.1, 37.2, 31.1, 19.3, 13.9. HRMS (ESI) calcd for  $\text{C}_{18}\text{H}_{25}\text{N}_3\text{O}_2$  [ $\text{M}+\text{H}$ ] $^+$  316.2020, found 316.2013.

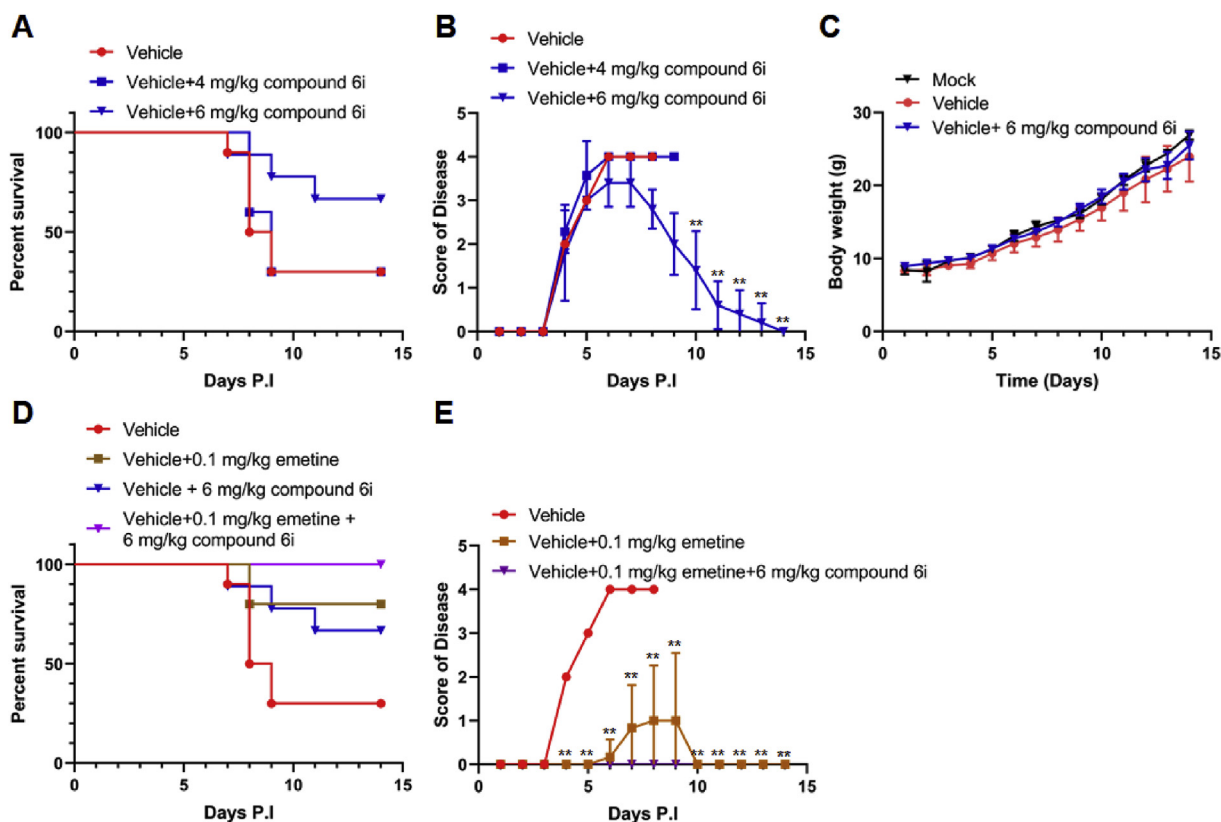


**Fig. 6.** Compound **6i** protected infected EV-A71 mice. Two-week-old KM mice ( $n = 10$ ) were infected with lethal strain of EV-A7 GZ-C11 using the IP route, and orally administrated with compound **6i** or emetine. Survival rates (6A) and clinical diseases (6B) were monitored daily after inoculation (\*\*:  $p < 0.001$ ; clinical scores compared between compound **6i** (4 mg/kg), compound **6i** (6 mg/kg) and vehicle); Body weight of KM ( $n = 10$ ) mice treated with compound **6i** (6C). Combination treatment with compound **6i** and emetine, compound **6i** increased the protective effect of emetine (6D, 6E) (\*\*:  $p < 0.001$ ; clinical scores compared between emetine (0.1 mg/kg), compound **6i** (6 mg/kg) + emetine (0.1 mg/kg) and vehicle). All treated groups were observed for lasting 14 days after infection.

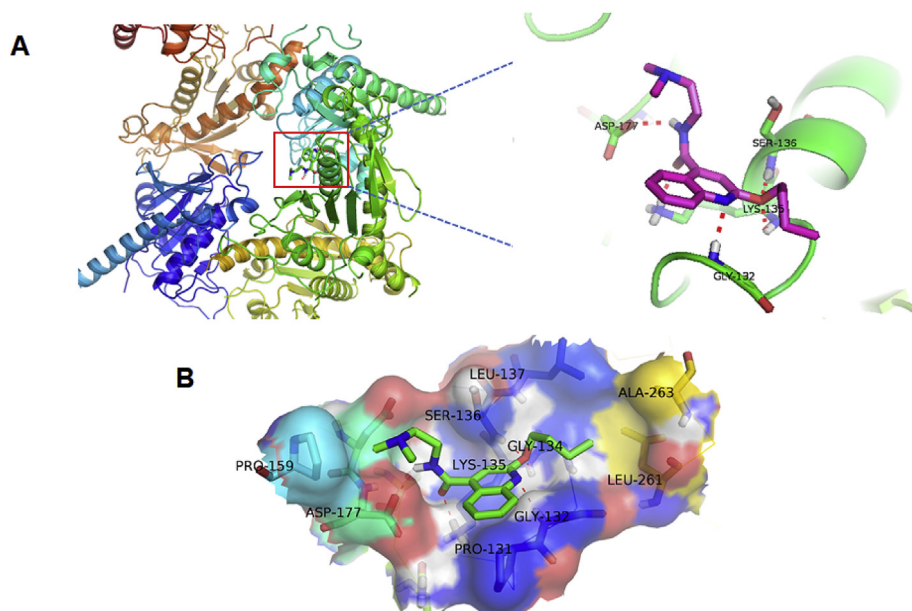


**Fig. 7.** Molecular docking experiment of **6i** bound into the EV-A71 2C protein. (A) An overview of the binding mode was displayed at a cartoon representation: binding site was expanded for **6i** and the C chain of 2C protein. Oxygen atom (red), Nitrogen atom (blue) and hydrogen bond was labeled with red dotted line. (B) Binding mode was showed in transparent ligand sites: Some key amino acids within 5 Å were labeled. (For interpretation of the references to colour in this figure legend, the reader is referred to the Web version of this article.)

4.2.4.10. *N*-(2-(Dimethylamino)ethyl)-2-(pentyloxy)quinoline-4-carboxamide (**6j**). White solid, 21.8% solid, mp 125–126 °C. <sup>1</sup>H NMR (400 MHz, CDCl<sub>3</sub>) δ 8.10 (d, *J* = 8.3 Hz, 1H), 7.84 (d, *J* = 8.3 Hz, 1H), 7.63 (s, 1H), 7.40 (t, *J* = 7.6 Hz, 1H), 6.97 (s, 1H), 6.85 (s, 1H), 4.47 (t, *J* = 6.7 Hz, 2H), 3.58 (q, *J* = 5.6 Hz, 2H), 2.55 (t, *J* = 5.9 Hz, 2H), 2.26 (s, 6H), 1.88–1.77 (m, 2H), 1.53–1.36 (m, 4H), 0.95 (t, *J* = 7.0 Hz, 3H). <sup>13</sup>C NMR (100 MHz, CDCl<sub>3</sub>) δ 167.2, 161.5, 147.3, 144.8, 129.9, 127.6, 125.3, 124.6, 121.5, 111.3, 66.3, 57.5, 45.0, 37.1, 28.7, 28.3, 22.5, 14.1. HRMS (ESI) calcd for C<sub>19</sub>H<sub>27</sub>N<sub>3</sub>O<sub>2</sub> [M+H]<sup>+</sup> 330.2176, found 330.2171.

4.2.4.11. *N*-(2-(Dimethylamino)ethyl)-2-(hexyloxy)quinoline-4-carboxamide (**6k**). White solid, 11.8% yield, mp 116–118 °C. <sup>1</sup>H NMR (400 MHz, CDCl<sub>3</sub>) δ 8.12 (d, *J* = 8.0 Hz, 1H), 7.85 (d, *J* = 8.3 Hz, 1H), 7.64 (t, *J* = 7.6 Hz, 1H), 7.41 (t, *J* = 7.6 Hz, 1H), 6.98 (s, 1H), 6.77 (s, 1H), 4.48 (t, *J* = 6.6 Hz, 2H), 3.66–3.50 (m, 2H), 2.58–2.50 (m, 2H), 2.26 (s, 6H), 1.91–1.74 (m, 2H), 1.49 (d, *J* = 7.8 Hz, 2H), 1.43–1.31 (m, 4H), 0.93 (t, *J* = 6.9 Hz, 3H). <sup>13</sup>C NMR (100 MHz, CDCl<sub>3</sub>) δ 167.2, 161.5, 147.3144.9, 129.9, 127.6, 125.3, 124.6, 121.6, 111.3, 66.3, 57.5, 45.1, 37.2, 31.6, 28.9, 25.8, 22.6, 14.1. HRMS (ESI) calcd for C<sub>20</sub>H<sub>29</sub>N<sub>3</sub>O<sub>2</sub> [M+H]<sup>+</sup> 344.2333, found 344.2325.

4.2.4.12. 2-Ethoxy-*N*-propylquinoline-4-carboxamide (**6l**). White solid, 67.2% yield, mp 163–165 °C. <sup>1</sup>H NMR (400 MHz, CDCl<sub>3</sub>) δ 8.04 (d, *J* = 7.7 Hz, 1H), 7.83 (d, *J* = 8.4 Hz, 1H), 7.64 (t, *J* = 7.7 Hz, 1H), 7.39 (t, *J* = 7.3 Hz, 1H), 6.90 (s, 1H), 6.26 (s, 1H), 4.53 (q, *J* = 7.0 Hz, 2H), 3.57–3.35 (m, 2H), 1.69–1.64 (m, 2H), 1.46 (t, *J* = 7.1 Hz, 3H), 1.01 (t, *J* = 7.4 Hz, 3H). <sup>13</sup>C NMR (100 MHz, CDCl<sub>3</sub>) δ 167.2, 161.3, 147.2, 145.1, 130.0, 127.6, 125.2, 124.6, 121.5, 111.0, 62.0, 41.7, 22.8, 14.5, 11.4. HRMS (ESI) calcd for C<sub>15</sub>H<sub>18</sub>N<sub>2</sub>O<sub>2</sub> [M+H]<sup>+</sup> 259.1441, found 259.1441.

4.2.4.13. 2-Propoxy-*N*-propylquinoline-4-carboxamide (**6m**). White solid, 72.2% yield, mp 157–159 °C. <sup>1</sup>H NMR (400 MHz, CDCl<sub>3</sub>) δ 8.05 (d, *J* = 8.8 Hz, 1H), 7.83 (d, *J* = 8.3 Hz, 1H), 7.64 (t, *J* = 8.3 Hz, 1H), 7.39 (t, *J* = 8.1 Hz, 1H), 6.92 (s, 1H), 6.22 (s, 1H), 4.43 (t, *J* = 6.7 Hz, 2H), 3.49–3.43 (m, 2H), 1.91–1.81 (m, 2H), 1.72–1.62 (m, 2H), 1.08 (t, *J* = 7.4 Hz, 3H), 1.02 (t, *J* = 7.4 Hz, 3H). <sup>13</sup>C NMR (100 MHz, CDCl<sub>3</sub>) δ 167.2, 161.5, 147.2, 145.1, 130.0, 127.6, 125.2, 124.6, 121.5, 111.0, 67.8, 41.7, 22.9, 22.3, 11.4, 10.6. HRMS (ESI) calcd for C<sub>16</sub>H<sub>20</sub>N<sub>2</sub>O<sub>2</sub> [M+H]<sup>+</sup> 273.1598, found 273.1596.

4.2.4.14. 2-Ethoxy-*N*-isobutylquinoline-4-carboxamide (**6n**). Yellow solid, 46.0% yield, mp 166–168 °C. <sup>1</sup>H NMR (400 MHz, CDCl<sub>3</sub>) δ 8.05 (d, *J* = 8.2 Hz, 1H), 7.84 (d, *J* = 8.3 Hz, 1H), 7.71–7.57 (m, 1H), 7.40 (t, *J* = 7.6 Hz, 1H), 6.92 (s, 1H), 6.23 (s, 1H), 4.54 (q, *J* = 7.1 Hz, 2H), 3.33 (t, *J* = 6.5 Hz, 2H), 1.98–1.86 (m, 1H), 1.46 (t, *J* = 7.1 Hz, 3H), 1.01 (d, *J* = 6.6 Hz, 6H). <sup>13</sup>C NMR (100 MHz, CDCl<sub>3</sub>) δ 167.2, 161.3, 147.3, 145.2, 130.0, 127.6, 125.2, 124.7, 121.5, 110.9, 62.0, 47.2, 28.6, 20.1, 14.5. HRMS (ESI) calcd for C<sub>16</sub>H<sub>20</sub>N<sub>2</sub>O<sub>2</sub> [M+H]<sup>+</sup> 273.1598, found 273.1596.

4.2.4.15. *N*-Isobutyl-2-propoxyquinoline-4-carboxamide (**6o**). White solid, 19.2% yield, mp 158–160 °C. <sup>1</sup>H NMR (400 MHz, CDCl<sub>3</sub>) δ 8.06 (d, *J* = 8.2 Hz, 1H), 7.84 (d, *J* = 8.4 Hz, 1H), 7.64 (t, *J* = 8.2 Hz, 1H), 7.40 (t, *J* = 7.6 Hz, 1H), 6.94 (s, 1H), 6.22 (s, 1H), 4.44 (t, *J* = 6.7 Hz, 2H), 3.34 (t, *J* = 6.5 Hz, 2H), 1.94 (dd, *J* = 13.5, 6.8 Hz, 1H), 1.90–1.81 (m, 2H), 1.08 (t, *J* = 7.4 Hz, 3H), 1.01 (d, *J* = 6.6 Hz, 6H). <sup>13</sup>C NMR (100 MHz, CDCl<sub>3</sub>) δ 167.2, 161.5, 147.2, 145.3, 130.1, 127.5, 125.2, 124.7, 121.5, 110.9, 67.9, 47.3, 28.6, 22.3, 20.2, 10.6. HRMS (ESI) calcd for C<sub>17</sub>H<sub>22</sub>N<sub>2</sub>O<sub>2</sub> [M+H]<sup>+</sup> 287.1754, found 287.1752.

4.2.4.16. *N*-Isobutyl-2-isopropoxyquinoline-4-carboxamide (**6p**). Yellow solid, 28.6% yield, mp 126–128 °C. <sup>1</sup>H NMR (400 MHz, CDCl<sub>3</sub>) δ 8.00 (d, *J* = 8.2 Hz, 1H), 7.81 (d, *J* = 8.3 Hz, 1H), 7.61 (t, *J* = 7.7 Hz, 1H), 7.35 (t, *J* = 8.0 Hz, 1H), 6.86 (s, 1H), 6.40 (s, 1H),

5.62–5.52 (m, 1H), 3.25 (t, *J* = 6.5 Hz, 2H), 1.91–1.80 (m, 1H), 1.41 (d, *J* = 6.2 Hz, 6H), 0.96 (d, *J* = 6.7 Hz, 6H). <sup>13</sup>C NMR (100 MHz, CDCl<sub>3</sub>) δ 167.3, 160.8, 147.3, 145.1, 129.9, 127.5, 125.2, 124.5, 121.3, 111.5, 68.4, 47.2, 28.6, 22.0, 20.1. HRMS (ESI) calcd for C<sub>17</sub>H<sub>22</sub>N<sub>2</sub>O<sub>2</sub> [M+H]<sup>+</sup> 287.1754, found 287.1751.

4.2.4.17. 2-Butoxy-*N*-(2-(pyrrolidin-1-yl)ethyl)quinoline-4-carboxamide (**6q**). Yellow thick liquid, 26.8% yield. <sup>1</sup>H NMR (400 MHz, CDCl<sub>3</sub>) δ 8.11 (d, *J* = 8.3 Hz, 1H), 7.84 (d, *J* = 8.4 Hz, 1H), 7.64 (t, *J* = 7.7 Hz, 1H), 7.40 (t, *J* = 7.7 Hz, 1H), 7.20 (s, 1H), 7.01 (s, 1H), 4.48 (t, *J* = 6.6 Hz, 2H), 3.71–3.62 (m, 2H), 2.84 (t, *J* = 5.6 Hz, 2H), 2.76–2.63 (m, 4H), 1.88–1.77 (m, 6H), 1.65–1.41 (m, 2H), 1.01 (t, *J* = 7.4 Hz, 3H). <sup>13</sup>C NMR (100 MHz, CDCl<sub>3</sub>) δ 167.3, 161.6, 147.3, 144.7, 129.9, 127.6, 125.3, 124.6, 121.6, 111.4, 66.0, 54.5, 53.9, 38.1, 31.0, 23.4, 19.3, 13.9. HRMS (ESI) calcd for C<sub>20</sub>H<sub>27</sub>N<sub>3</sub>O<sub>2</sub> [M+H]<sup>+</sup> 342.2176, found 342.2168.

4.2.4.18. 2-Butoxy-*N*-(2-(piperidin-1-yl)ethyl)quinoline-4-carboxamide (**6r**). Yellow solid, 45.9% yield, mp 100–103 °C. <sup>1</sup>H NMR (400 MHz, CDCl<sub>3</sub>) δ 8.09 (d, *J* = 8.3 Hz, 1H), 7.84 (d, *J* = 8.3 Hz, 1H), 7.62 (t, *J* = 7.7 Hz, 1H), 7.38 (t, *J* = 7.6 Hz, 1H), 6.95 (s, 1H), 6.89 (s, 1H), 4.47 (t, *J* = 6.7 Hz, 2H), 3.56 (q, *J* = 5.7 Hz, 2H), 2.53 (t, *J* = 6.1 Hz, 2H), 2.40 (s, 4H), 1.91–1.69 (m, 2H), 1.62–1.48 (m, 6H), 1.48–1.32 (m, 2H), 1.01 (t, *J* = 7.4 Hz, 3H). <sup>13</sup>C NMR (100 MHz, CDCl<sub>3</sub>) δ 167.1, 161.6, 147.3, 145.0, 129.9, 127.6, 125.3, 124.5, 121.5, 111.3, 66.0, 57.0, 54.3, 36.6, 31.0, 25.9, 24.3, 19.3, 13.9. HRMS (ESI) calcd for C<sub>21</sub>H<sub>29</sub>N<sub>3</sub>O<sub>2</sub> [M+H]<sup>+</sup> 356.2333, found 356.2325.

4.2.4.19. 2-Butoxy-*N*-(3-(dimethylamino)propyl)quinoline-4-carboxamide (**6s**). White solid, 18.4% yield, mp 91–94 °C. <sup>1</sup>H NMR (400 MHz, CDCl<sub>3</sub>) δ 8.14 (d, *J* = 8.5 Hz, 1H), 8.11 (s, 1H), 7.84 (d, *J* = 8.3 Hz, 1H), 7.63 (t, *J* = 8.2 Hz, 1H), 7.39 (t, *J* = 7.2 Hz, 1H), 6.94 (s, 1H), 4.48 (t, *J* = 6.7 Hz, 2H), 3.59 (q, *J* = 5.8 Hz, 2H), 2.50 (t, *J* = 6.2 Hz, 2H), 2.22 (s, 6H), 1.86–1.77 (m, 4H), 1.58–1.39 (m, 2H), 1.00 (t, *J* = 7.4 Hz, 3H). <sup>13</sup>C NMR (100 MHz, CDCl<sub>3</sub>) δ 167.0, 161.6, 147.3, 145.2, 129.9, 127.5, 125.4, 124.5, 121.6, 111.1, 66.0, 58.7, 45.2, 40.1, 31.0, 25.5, 19.3, 13.9. HRMS (ESI) calcd for C<sub>19</sub>H<sub>27</sub>N<sub>3</sub>O<sub>2</sub> [M+H]<sup>+</sup> 330.2176, found 330.2169.

4.2.4.20. 2-Butoxy-*N*-(3-(diethylamino)propyl)quinoline-4-carboxamide (**6t**). Yellow thick liquid, 20.1% yield. <sup>1</sup>H NMR (400 MHz, CDCl<sub>3</sub>) δ 8.50 (s, 1H), 8.14 (d, *J* = 8.2 Hz, 1H), 7.84 (d, *J* = 8.3 Hz, 1H), 7.63 (t, *J* = 7.7 Hz, 1H), 7.39 (t, *J* = 7.6 Hz, 1H), 6.97 (d, *J* = 2.1 Hz, 1H), 4.47 (t, *J* = 6.6 Hz, 2H), 3.62 (d, *J* = 6.1 Hz, 2H), 2.72 (s, 2H), 2.63–2.51 (m, 4H), 1.92–1.84 (m, 2H), 1.80 (q, *J* = 7.0 Hz, 2H), 1.53–1.48 (m, 2H), 1.01 (d, *J* = 7.4 Hz, 3H), 0.97 (t, *J* = 5.4 Hz, 6H). <sup>13</sup>C NMR (100 MHz, CDCl<sub>3</sub>) δ 167.2, 161.6, 147.3, 145.0, 129.9, 127.5, 125.4, 124.5, 121.6, 111.2, 65.9, 46.4, 39.9, 31.0, 24.6, 19.3, 13.9, 10.6. HRMS (ESI) calcd for C<sub>21</sub>H<sub>31</sub>N<sub>3</sub>O<sub>2</sub> [M+H]<sup>+</sup> 358.2489, found 358.2480.

### 4.3. Biological assays

#### 4.3.1. Cells, antibodies and viruses

RD cells, Vero cells, EV-A71, EV-A71 VP1 antibody (10F0) and Tubulin (T5168) were used in this study as previously reported [33]. An anti-dsRNA antibody (MABE1134) and an EV-A71 2C polyclonal antibody (GTX132354) for immunofluorescence assay or Western blot were purchased from Merck and GeneTex, respectively.

#### 4.3.2. Cytotoxicity assay

A CCK8 kit (YEASEN, China) was applied to evaluate the cell viability as previously reported [33].

#### 4.3.3. Immunofluorescence (IF)

For immunofluorescence assay, the procedures are described in our previous study [33]. In short, 4% paraformaldehyde was applied to fix RD or Vero cells, then permeabilized with PBS containing 0.2% Triton X-100 for 5 min; then incubated overnight with EV-A71 VP1 or 2C or dsRNA antibody at 4 °C and subsequently incubated with secondary antibodies for 1 h, and then stained with 4' 6-diamidino-2-phenylindole (DAPI) solution (Beyotime, C1002) with indicated concentration (5 µg/ml) in PBS for 5 min. Finally, cells were examined on a Leica confocal microscope.

#### 4.3.4. Nucleic acid helix unwinding and strand hybridization assays

The helix destabilizing assay and the RNA strand hybridization assay was conducted following a standard protocol as previously reported [27]. The reaction mixture with compound **6i** or DMSO was prepared as in Table S1. The HEX-labeled RNA and complementary RNA were synthesized as listed in Table S2, respectively.

#### 4.3.5. Western blot

Western blot assay was conducted following a protocol as previously reported [33].

#### 4.3.6. Plaque assay

Plaque assay was carried out according to a standard protocol [35]. The calculation of EC<sub>50</sub> based on nonlinear regression using the GraphPad Prism 8.0, as in reported work [36].

#### 4.3.7. qRT-PCR

RNA extraction, cDNA synthesis, qRT-PCR and viral RNA titer quantitation was performed as previously reported [33]. The EV-A71-specific primers for qRT-PCR were listed in Table S2.

#### 4.3.8. Time-of-addition assay

A time-of-addition assay was applied to assess the life stage of EV-A71 compound **6i** inhibition as reported [33]. In short, RD or Vero cells were infected with EV-A71 at 1 MOI, then cells were treated with compound **6i** or enviroxime or DMSO at indicated timepoints. Cell lysis or supernatants were collected for Western blot or RT-PCR analysis at 12 hpi.

#### 4.3.9. Mouse infection study

The antiviral effect of compound **6i** *in vivo* was evaluated as previously reported [37]. Briefly, Two-week-old KM mice were purchased from HuBei Center for Disease Control (CDC) (Wuhan, China) and were infected with highly virulent EV-A71 (GZ-CII strain) by intraperitoneal (IP) injection at a lethal dose. All animal experiments comply with the animal welfare guidelines (NIH Publications No. 8023, revised 1978). Doses of compound **6i** at 4 or 6 mg/kg or emetine at 0.1 mg/kg (positive control) initiated 6 h before challenge and continuing for 4 days [33,38]. Uninfected or infected mice treated with the vehicle alone were designed as control groups. All mice were monitored and weighed daily, and survival rates and clinical diseases were recorded for consecutive at least 14 days. KM mice were infected with highly virulent EV-A71 (GZ-CII strain) by IP injection at a lethal dose of  $0.8 \times 10^8$  pfu and  $1.2 \times 10^8$  pfu for the determination of survival rates and clinical diseases, respectively. Clinical score definition as followings: Healthy, 0 point; Lethargy and inactivity, limb weakness, 1 point; Less exercise, limb paralysis, 2 points; Quadriplegic, moribund, 3 points; Death, 4 points. And to minimize the pain of mice, when two-limb paralysis and dying was observed, the mice were euthanized.

#### 4.3.10. Molecular modeling

The crystal structure of EV-A71 2C protein (PDB ID: 5GQ1) [28] was download from the PDB website and pretreated with PyMOL.

Then AutoDock software was applied to dock the compound **6i** into the structure of EV-A71 2C protein. Chem3D Pro 14.0 was used to calculated the minimal energy of this compounds and saved as pdb format. During the docking, the box was set as 100 Å, 100 Å, and 120 Å in the X, Y and Z dimensions, respectively. The obtained complex was analyzed and the figures were obtained by PyMOL.

#### Author contributions

The manuscript was written through contributions of all authors. All authors have given approval to the final version of the manuscript.

#### Declaration of competing interest

The authors declare that they have no known competing financial interests or personal relationships that could have appeared to influence the work reported in this paper.

#### Acknowledgment

We thank Dr. Xi Zhou for generously providing pFastBacHTB-MBP-EV71 2CATPase; Dr. Tao Peng (Guangzhou, China) for EV-A71 GZ-CII mice adapted virus. This study was supported by the NSFC (81971976, 81773557, 81772236), Major Project of Technology Innovation Program of Hubei Province (2018ACA123).

#### Appendix A. Supplementary data

Supplementary data to this article can be found online at <https://doi.org/10.1016/j.ejmech.2020.112310>.

#### Ethics

All the animal experimentation was approved by Ethics Committee of Wuhan University (Wuhan, China).

#### References

- [1] J. Baggen, H.J. Thibaut, J.R.P.M. Strating, F.J.M. van Kuppeveld, The life cycle of non-polio enteroviruses and how to target it, *Nat. Rev. Microbiol.* 16 (2018) 368–381.
- [2] T.-Y. Lin, L.-Y. Chang, S.-H. Hsia, Y.-C. Huang, C.-H. Chiu, C. Hsueh, S.-R. Shih, C.-C. Liu, M.-H. Wu, The 1998 enterovirus 71 outbreak in Taiwan: pathogenesis and management, *Clin. Infect. Dis.* 34 (2002) S52–S57.
- [3] B. Yang, F. Liu, Q. Liao, P. Wu, Z. Chang, J. Huang, L. Long, L. Luo, Y. Li, G.M. Leung, B.J. Cowling, H. Yu, Epidemiology of hand, foot and mouth disease in China, 2008 to 2015 prior to the introduction of EV-A71 vaccine, *Euro Surveill.* 22 (2017), 16-00824.
- [4] M.H. Ooi, S.C. Wong, P. Lewthwaite, M.J. Cardosa, T. Solomon, Clinical features, diagnosis, and management of enterovirus 71, *Lancet Neurol.* 9 (2010) 1097–1105.
- [5] L.-Y. Chang, T.-Y. Lin, K.-H. Hsu, Y.-C. Huang, K.-L. Lin, C. Hsueh, S.-R. Shih, H.-C. Ning, M.-S. Hwang, H.-S. Wang, C.-Y. Lee, Clinical features and risk factors of pulmonary oedema after enterovirus-71-related hand, foot, and mouth disease, *Lancet* 354 (1999) 1682–1686.
- [6] N.J. Schmidt, E.H. Lennette, H.H. Ho, An apparently new enterovirus isolated from patients with disease of the central nervous system, *Clin. Infect. Dis.* 129 (1974) 304–309.
- [7] P.-C. Chang, S.-C. Chen, K.-T. Chen, The current status of the disease caused by enterovirus 71 infections: epidemiology, pathogenesis, molecular epidemiology, and vaccine development, *Int. J. Environ. Res. Publ. Health* 13 (2016) 890.
- [8] M. Ho, E.-R. Chen, K.-H. Hsu, S.-J. Twu, K.-T. Chen, S.-F. Tsai, J.-R. Wang, S.-R. Shih, An epidemic of enterovirus 71 infection in Taiwan, *N. Engl. J. Med.* 341 (1999) 929–935.
- [9] F. Zhu, W. Xu, J. Xia, Z. Liang, Y. Liu, X. Zhang, X. Tan, L. Wang, Q. Mao, J. Wu, Y. Hu, T. Ji, L. Song, Q. Liang, B. Zhang, Q. Gao, J. Li, S. Wang, Y. Hu, S. Gu, J. Zhang, G. Yao, J. Gu, X. Wang, Y. Zhou, C. Chen, M. Zhang, M. Cao, J. Wang, H. Wang, N. Wang, Efficacy, safety, and immunogenicity of an enterovirus 71 vaccine in China, *N. Engl. J. Med.* 370 (2014) 818–828.
- [10] R. Li, L. Liu, Z. Mo, X. Wang, J. Xia, Z. Liang, Y. Zhang, Y. Li, Q. Mao, J. Wang, L. Jiang, C. Dong, Y. Che, T. Huang, Z. Jiang, Z. Xie, L. Wang, Y. Liao, Y. Liang,

- Y. Nong, J. Liu, H. Zhao, R. Na, L. Guo, J. Pu, E. Yang, L. Sun, P. Cui, H. Shi, J. Wang, Q. Li, An inactivated enterovirus 71 vaccine in Healthy children, *N. Engl. J. Med.* 370 (2014) 829–837.
- [11] P. Chong, C.C. Liu, Y.H. Chow, A.H. Chou, M. Klein, Review of enterovirus 71 vaccines, *Clin. Infect. Dis.* 60 (2015) 797–803.
- [12] Y. Ma, C. Shang, P. Yang, L. Li, Y. Zhai, Z. Yin, B. Wang, L. Shang, 4-Iminoxazolidin-2-one as a bioisostere of the cyanohydrin moiety: inhibitors of enterovirus 71 3C protease, *J. Med. Chem.* 61 (2018) 10333–10339.
- [13] E. Wimmer, C.U.T. Hellen, X. Cao, Genetics of poliovirus, *Annu. Rev. Genet.* 27 (1993) 353–436.
- [14] X. Wang, W. Peng, J. Ren, Z. Hu, J. Xu, Z. Lou, X. Li, W. Yin, X. Shen, C. Porta, T.S. Walter, G. Evans, D. Axford, R. Owen, D.J. Rowlands, J. Wang, D.I. Stuart, E.E. Fry, Z. Rao, A sensor-adaptor mechanism for enterovirus uncoating from structures of EV71, *Nat. Struct. Mol. Biol.* 19 (2012) 424–429.
- [15] D.C. Pevear, T.M. Tull, M.E. Seipel, J.M. Groarke, Activity of Pleconaril against enteroviruses, *Antimicrob. Agents Chemother.* 43 (1999) 2109–2115.
- [16] H.A. Rotbart, A.D. Webster, Treatment of potentially life-threatening enterovirus infections with Pleconaril, *Clin. Infect. Dis.* 32 (2001) 228–235.
- [17] F.G. Hayden, D.T. Herrington, T.L. Coats, K. Kim, E.C. Cooper, S.A. Villano, S. Liu, S. Hudson, D.C. Pevear, M. Collett, M. McKinlay, Pleconaril respiratory infection study, efficacy and safety of oral Pleconaril for treatment of colds due to picornaviruses in adults: results of 2 double-blind, randomized, placebo-controlled trials, *Clin. Infect. Dis.* 36 (2003) 1523–1532.
- [18] F. Russell, K. Laessig, Safety and efficacy evaluation of Pleconaril for treatment of the common cold, *Clin. Infect. Dis.* 37 (2003), 1722–1722.
- [19] A.M. MacLeod, D.R. Mitchell, N.J. Palmer, H. Van de Poël, K. Conrath, M. Andrews, P. Leyssen, J. Neyts, Identification of a series of compounds with potent antiviral activity for the treatment of enterovirus infections, *ACS Med. Chem. Lett.* 4 (2013) 585–589.
- [20] H.M. van der Schaar, L. van der Linden, K.H.W. Lanke, J.R.P.M. Strating, G. Pürstinger, E. de Vries, C.A.M. de Haan, J. Neyts, F.J.M. van Kuppeveld, Coxsackievirus mutants that can bypass host factor PI4KIII $\beta$  and the need for high levels of PI4P lipids for replication, *Cell Res.* 22 (2012) 1576–1592.
- [21] F. Victor, R. Loncharich, J. Tang, W.A. Spitzer, Synthesis and antiviral activity of C2 analogs of Enviroxime: an exploration of the role of critical functionality, *J. Med. Chem.* 40 (1997) 3478–3483.
- [22] R.J. Phillpotts, J. Wallace, D.A. Tyrrell, V.B. Tagart, Therapeutic activity of enviroxime against rhinovirus infection in volunteers, *Antimicrob. Agents Chemother.* 23 (1983) 671–675.
- [23] P.-H. Hsyu, Y.K. Pithavala, M. Gersten, C.A. Penning, B.M. Kerr, Pharmacokinetics and safety of an antirhinoviral agent, rupintrivir, in Healthy volunteers, *antimicrob. Agents Chemother.* 46 (2002) 392–397.
- [24] A.K. Patick, M.A. Brothers, F. Maldonado, S. Binford, O. Maldonado, S. Fuhrman, A. Petersen, G.J. Smith, L.S. Zalman, L.A. Burns-Naas, J.Q. Tran, In vitro antiviral activity and single-dose pharmacokinetics in humans of a novel, orally bioavailable inhibitor of human rhinovirus 3C protease, *Antimicrob. Agents Chemother.* 49 (2005) 2267–2275.
- [25] J.-H. Song, S.-R. Kim, E.-Y. Heo, J.-Y. Lee, D.-e. Kim, S. Cho, S.-Y. Chang, B.-I. Yoon, J. Seong, H.-J. Ko, Antiviral activity of gemcitabine against human rhinovirus in vitro and in vivo, *Antivir. Res.* 145 (2017) 6–13.
- [26] C.-L. Deng, H. Yeo, H.-Q. Ye, S.-Q. Liu, B.-D. Shang, P. Gong, S. Alonso, P.-Y. Shi, B. Zhang, Inhibition of enterovirus 71 by adenosine analog NITD008, *J. Virol.* 88 (2014) 11915–11923.
- [27] H. Xia, P. Wang, G.-C. Wang, J. Yang, X. Sun, W. Wu, Y. Qiu, T. Shu, X. Zhao, L. Yin, C.-F. Qin, Y. Hu, X. Zhou, Human enterovirus nonstructural protein 2CATPase functions as both an RNA helicase and ATP-independent RNA chaperone, *PLoS Pathog.* 11 (2015), e1005067.
- [28] H. Guan, J. Tian, B. Qin, J.A. Wojdyla, B. Wang, Z. Zhao, M. Wang, S. Cui, Crystal structure of 2C helicase from enterovirus 71, *Sci Adv* 3 (2017), e1602573.
- [29] X. Han, N. Sun, H. Wu, D. Guo, P. Tien, C. Dong, S. Wu, H.-B. Zhou, Identification and structure–activity relationships of diarylhydrazides as novel potent and selective human enterovirus inhibitors, *J. Med. Chem.* 59 (2016) 2139–2150.
- [30] J. Pan, X. Han, N. Sun, H. Wu, D. Lin, P. Tien, H.-B. Zhou, S. Wu, Synthesis of N-benzyl-N-phenylthiophene-2-carboxamide analogues as a novel class of enterovirus 71 inhibitors, *RSC Adv.* 5 (2015) 55100–55108.
- [31] R. Ulferts, S.M. de Boer, L. van der Linden, L. Bauer, H.R. Lyoo, M.J. Maté, J. Lichière, B. Canard, D. Lelieveld, W. Omta, D. Egan, B. Coutard, F.J.M. van Kuppeveld, Screening of a library of FDA-approved drugs identifies several enterovirus replication inhibitors that target viral protein 2C, *Antimicrob. Agents Chemother.* 60 (2016) 2627–2638.
- [32] R. Musharrafi, J. Zhang, P. Tuohy, N. Kitamura, S.S. Bellampalli, Y. Hu, R. Khanna, J. Wang, Discovery of quinoline analogues as potent antivirals against enterovirus D68 (EV-D68), *J. Med. Chem.* 62 (2019) 4074–4090.
- [33] Q. Tang, S. Li, L. Du, S. Chen, J. Gao, Y. Cai, Z. Xu, Z. Zhao, K. Lan, S. Wu, Emetine protects mice from enterovirus infection by inhibiting viral translation, *Antivir. Res.* 173 (2020), 104650.
- [34] J. Zuo, K.K. Quinn, S. Kye, P. Cooper, R. Damoiseaux, P. Krogstad, Fluoxetine is a potent inhibitor of coxsackievirus replication, *Antimicrob. Agents Chemother.* 56 (2012) 4838–4844.
- [35] A. Au - Baer, K. Au - Kehn-Hall, Viral concentration determination through plaque assays: using traditional and novel overlay systems, *JoVE* (2014), e52065.
- [36] L.V. Pham, S.B. Jensen, U. Fahnøe, M.S. Pedersen, Q. Tang, L. Ghanem, S. Ramirez, D. Humes, S.B.N. Serre, K. Schønning, J. Bukh, J.M. Gottwein, HCV genotype 1-6 NS3 residue 80 substitutions impact protease inhibitor activity and promote viral escape, *J. Hepatol.* 70 (2019) 388–397.
- [37] Y. Xu, S. Ma, L. Zhu, Z. Huang, L. Chen, Y. Xu, H. Yin, T. Peng, Y. Wang, Clinically isolated enterovirus A71 subgroup C4 strain with lethal pathogenicity in 14-day-old mice and the application as an EV-A71 mouse infection model, *Antivir. Res.* 137 (2017) 67–75.
- [38] M.J.P. van Dongen, R.U. Kadam, J. Juraszek, E. Lawson, B. Brandenburg, F. Schmitz, W.B.G. Schepens, B. Stoops, H.A. van Diepen, M. Jongeneelen, C. Tang, J. Vermond, A. van Eijgen-Obregoso Real, S. Blokland, D. Garg, W. Yu, W. Goutier, E. Lanckacker, J.M. Klap, D.C.G. Peeters, J. Wu, C. Buyck, T.H.M. Jonckers, D. Roymans, P. Roevens, R. Vogels, W. Koudstaal, R.H.E. Friesen, P. Raboisson, D. Dhanak, J. Goudsmit, I.A. Wilson, A small-molecule fusion inhibitor of influenza virus is orally active in mice, *Science* 363 (2019) eaar6221.